

10534 5614 NT ACAN

NACA
TN
4195
e.1

006683



TECH LIBRARY KAFB, NM

NATIONAL ADVISORY COMMITTEE FOR AERONAUTICS

TECHNICAL NOTE 4195 LOAN COPY: RETURN TO
AFWL TECHNICAL LIBRARY
KIRTLAND AFB, N. M.

SHAPE OF INITIAL PORTION OF BOUNDARY
OF SUPERSONIC AXISYMMETRIC FREE JETS
AT LARGE JET PRESSURE RATIOS

By Eugene S. Love and Louise P. Lee

Langley Aeronautical Laboratory
Langley Field, Va.



Washington

January 1958



0066883

TECHNICAL NOTE 4195

SHAPE OF INITIAL PORTION OF BOUNDARY
OF SUPERSONIC AXISYMMETRIC FREE JETS
AT LARGE JET PRESSURE RATIOS

By Eugene S. Love and Louise P. Lee

SUMMARY

Calculations have been made of the initial portion of the boundary of axisymmetric free jets exhausting at large ratios of jet static pressure to stream static pressure from a conically divergent nozzle having a jet exit Mach number of 2.5 and a semidivergence angle of 15° . The results of the calculations indicate the size and shape of the jet to be expected at large pressure ratios, the effects of the ratio of specific heats, and the large initial inclinations of the boundary that are likely to be encountered by hypersonic vehicles at high altitude.

INTRODUCTION

In the proposed trajectories of most rocket-propelled hypersonic vehicles, the rocket propulsion unit will remain in operation long enough for the exhausting jet to encounter the very low pressures of high altitudes. When this condition occurs, the ratio of the jet static pressure to stream static pressure becomes very large at the nozzle exit, and as a result the free jet expands greatly. The problems created by the presence of this large, bulbous, free jet of gases immediately downstream of the nozzle exit are, in the main, twofold. First, the large deflections of the free-stream flow caused by the jet flow may result in major aerodynamic interference upon nearby surfaces; for example, large regions of separated flow may be created on the vehicle surface ahead of the rocket exit. Second, the heat existing in the core of this large mass of gases may at hypersonic speeds introduce direct heating problems through radiation by causing the temperatures of the nearby surfaces which are already experiencing high aerodynamic heating to exceed the critical values. None of the aerodynamic interference effects can be estimated with any reliability without some idea of the magnitude of the region encompassed by the free jet and the shape of its boundary.

For the purpose of gaining insight into the size and shape of free jets at large pressure ratios, a number of calculations have been made of the initial portion of the boundary of axisymmetric free jets exhausting into still air for jet static-pressure ratios ranging from about 60 to 42,000 for ratios of specific heat of 1.200, 1.400, and 1.667. All calculations of the jet boundaries were made for a conically divergent nozzle having a semidivergence angle of 15° and a Mach number of 2.5 for the jet flow at the nozzle surface immediately ahead of the exit.

SYMBOLS

The symbol notation that follows will be clarified by reference to the flow diagram shown in figure 1.

M_j	jet Mach number; value at nozzle surface immediately ahead of exit
M_∞	free-stream Mach number; also Mach number ahead of exit shock or ahead of shock at beginning of separation
p_∞	ambient or free-stream static pressure; also pressure ahead of exit shock or ahead of shock at beginning of separation
p_j	jet static pressure; value at nozzle surface immediately ahead of exit
p'_∞	static pressure of external flow existing immediately ahead of jet exit and behind exit shock, or pressure in region of separated flow immediately ahead of jet exit
r_j	radius of jet exit
x	distance from plane of nozzle exit measured parallel to jet axis
y	perpendicular distance from jet axis
γ_j	ratio of specific heat at constant pressure to specific heat at constant volume for jet flow
δ_j	initial inclination of free-jet boundary at exit
θ_N	semidivergence angle of conically divergent nozzle

CALCULATION OF BOUNDARIES

General Procedure

The method of characteristics was used throughout to calculate the jet boundaries. Leading characteristic lines (see fig. 1) and the initial values for the characteristic lines from the center of expansion were computed manually. The characteristic nets were determined on a card-programmed electronic calculator. For expediency, only the boundary points and a portion of the characteristic net sufficient to define the jet shock (by the foldback method of characteristics) were retained in the print-out phase of the automatic calculations.

Although considerable experience had been obtained at the Langley Laboratory in previous calculations of jet boundaries for low static-pressure ratios (of the order of 10 and lower), no information was available for determining beforehand the increments between the characteristic lines introduced from the center of expansion that should be used to insure a reliable boundary solution for the large pressure ratios of this study. A similar situation existed as regards the spacing of the points along the leading characteristic line. After some trial calculations of boundaries, it was decided to introduce a new characteristic line from the center of expansion for approximately every degree of expansion. The spacing of the points along the leading characteristic line was selected on the basis of additional trial calculations and other factors, some of which are discussed subsequently in the section "Presentation of Boundaries." However, it may be noted here that points along the leading characteristic line were calculated for increments in x/r_j of 0.02, and this spacing is recommended for the range of pressure ratios covered by this study. For values of M_j and θ_N greatly different from the values used herein ($M_j = 2.5$, $\theta_N = 15^\circ$), and for pressure ratios greater than those covered in this study (of the order of 42,000), the rate at which the characteristic lines were introduced from the center of the expansion and the point spacing used along the leading characteristic line might not be adequate. With regard to the latter, the shape and inclination of the leading characteristic line have, in general, first-order dependence upon M_j and θ_N .

Static-Pressure Ratios for Calculations

The choice of static-pressure ratios for the calculations was influenced to some extent by an examination of the variation of the initial inclination of the jet boundary δ_j (see fig. 1) with static-pressure ratio p_j/p_∞ . This variation is presented in figure 2 for

the values of the ratio of specific heats γ_j used in the boundary calculations. It is interesting to note first the magnitude of δ_j for the nozzle with a sonic exit ($M_j = 1$, $\theta_N = 0^\circ$), since at very large values of p_j/p_∞ this nozzle gives the largest possible values of δ_j (fig. 2). By comparison with these values for the sonic nozzle, the values of δ_j for the nozzle of this study ($M_j = 2.5$, $\theta_N = 15^\circ$) are significantly lower at very large values of p_j/p_∞ , and this difference increases with decreasing γ_j . Of course at very low values of p_j/p_∞ any conically divergent nozzle will produce a value of δ_j greater than that for the sonic nozzle, since $\delta_j = \theta_N$ at $p_j/p_\infty = 1$; in this instance, $\delta_j = \theta_N = 15^\circ$ for $p_j/p_\infty = 1$.

The curves of figure 2 illustrate that, at large values of p_j/p_∞ , conically divergent nozzles likely to be encountered in practical applications may produce large initial inclinations of the boundary. For rockets where γ_j is of the order of 1.2 and sometimes less, this initial inclination may easily exceed 90° , and at extremely large pressure ratios it is not inconceivable for the free-jet flow at the jet boundary to be directed initially almost 180° opposite to the direction of flow along the jet axis. Thus, to the general objective of gaining some familiarity with the size and shape of free jets at large pressure ratios is added the objective of calculating some boundaries for which $\delta_j > 90^\circ$. In addition, boundaries for which a comparison will show the effects of γ_j for similar values of p_j/p_∞ and for similar values of δ_j are desired.

The curves of figure 2 show that the variation of δ_j with p_j/p_∞ is such that at p_j/p_∞ of the order of 10^8 for $\gamma_j = 1.667$ and of the order of 10^{22} for $\gamma_j = 1.200$, the initial inclination has approached closely its maximum value. Consequently, if calculations could be made near these values of p_j/p_∞ (or higher), they should be sufficient for most purposes to represent jets operating in the range from these values to infinity. Unfortunately, although solutions were attempted for these extremely large pressure ratios, satisfactory results could not be obtained without successive refinements and reprogramming of the automatic calculations. For these reasons and because of other commitments

of the electronic calculators, the boundaries at these extremely large pressure ratios were not obtained. The values of p_j/p_∞ , and the corresponding values of δ_j , for which boundaries were calculated are given in the following table (boundaries for p_j/p_∞ of the order of 10 and less were available from previous calculations):

$\gamma_j = 1.667$		$\gamma_j = 1.400$		$\gamma_j = 1.200$	
p_j/p_∞	δ_j , deg	p_j/p_∞	δ_j , deg	p_j/p_∞	δ_j , deg
59.92	48.55	81.94	60.02	76.58	70.99
569.2	57.72	1,346	75.59	1,303	94.51
1,618	60.74	2,692	78.53	9,776	107.6
				41,820	115.6

The exact values of p_j/p_∞ used in the calculations were determined by the arbitrary condition of terminating the expansion at one of the manually calculated characteristic lines from the center of expansion.

RESULTS AND DISCUSSION

Presentation of Boundaries

The calculated boundaries are presented in the form of curves with discontinuous slopes; this type of presentation is compatible with the lattice-point characteristic method (that is, calculated points on boundary joined by straight lines). In practical applications a smooth curve is, of course, fitted to the discontinuous-slope form of the boundary, particular care being taken to maintain the initial inclination of the boundary.

Separate presentation with jet shocks.— The calculated boundaries together with the indicated position of the shock formed within the jet (given by the intersection and coalescence of characteristic lines of the same family) are shown separately for each value of p_j/p_∞ in figures 3 to 5. For $\gamma_j = 1.200$, only the boundary for $p_j/p_\infty = 76.58$ is presented separately (fig. 5) inasmuch as only a minute segment of the jet shock was indicated in the inadvertently shortened calculation at $p_j/p_\infty = 1,303$, and none was indicated at the higher values of p_j/p_∞ .

All boundaries for $\gamma_j = 1.200$, as well as for the other values of γ_j , are presented together subsequently. At first glance the results for all values of γ_j give indication of a tendency for the jet shock to be eliminated with increasing p_j/p_∞ at large p_j/p_∞ . It would, however, appear debatable as to whether a valid indication of such an occurrence could be substantiated by these calculations, inasmuch as an inherent stretching of the meshes within the characteristic net occurs with increasing p_j/p_∞ in these calculations. Nevertheless, it may be reasoned that for $p_j/p_\infty = \infty$ the velocity at the boundary is radial; that is, the characteristic line is in the same direction as the direction of the velocity, which is the direction of the boundary. Consequently, the only coalescence of the characteristic lines occurs on the boundary. It follows that if at $p_j/p_\infty = \infty$ this coalescence were indicative of a shock, the shock would coincide with the boundary. However, since a shock must have a pressure rise across it, the existence of a shock on the boundary represents an impossible condition for $p_j/p_\infty = \infty$ in view of the following: first, a pressure rise cannot exist across a boundary, and second, the existence of a pressure rise at $p_j/p_\infty = \infty$ would imply that, in expanding to a vacuum, the jet flow has expanded to a pressure less than a vacuum and thus requires a pressure rise at the boundary to restore its pressure to the ambient vacuum, a clearly impossible situation. Thus, it appears that at $p_j/p_\infty = \infty$ no jet shock will be present, and an indication of the elimination of the jet shock with increasing p_j/p_∞ may, at large p_j/p_∞ , be reasonable.

In figures 4(a) and 5, two boundaries and two shocks are shown. In both figures these two boundaries and shocks represent the examination of the effect of point spacing along the leading characteristic line upon the shape and position of the calculated boundary and the jet shock. This examination was primarily an outgrowth of the desire to retain a programing capacity (30 points along the leading characteristic) for the automatic calculations that had been used in previous studies at lower pressure ratios and, at the same time, to obtain, if possible, a significant portion of the boundary and jet shock without incurring large errors. The shorter boundaries and jet shocks correspond to calculations made by the use of the first 30 points along the leading characteristic (that is, increments in x/r_j maintained standard at 0.02). The longer boundaries and jet shocks correspond to results obtained by use of every other point of the first 30 calculated points on the leading characteristic (increments in x/r_j of 0.04), every third point of the second 30 (increments in x/r_j of 0.06), and every fourth point of an

additional 20 (increments in x/r_j of 0.08). The results show that the errors associated with the larger point spacing are small; consequently this spacing was used in most of the calculations. In these figures and those to follow, a few of the boundaries do not have the extent to be expected from this point spacing. For these boundaries, difficulties encountered in the automatic phase of the calculation shortened the calculations. Since with one or two exceptions the completed portions of the boundaries for these shortened calculations are believed to convey adequately the shape of the boundary over a considerable distance from the jet exit, no effort was made to continue these calculations.

Composite presentation.- In figure 6, the boundaries for each value of γ_j are presented compositely to show more readily the effect of increasing p_j/p_∞ . Included are boundaries for $p_j/p_\infty = 1$ and 10 calculated in a previous study. The enormous size that the free jet may attain at large pressure ratios is readily apparent, particularly at $\gamma_j = 1.200$ (fig. 6(c)) when the initial inclination of the boundary approaches and exceeds the vertical.

Effect of γ_j

Effect of γ_j for essentially equal pressure ratios.- Some idea of the effect of γ_j at large pressure ratios upon the shape of the boundary for essentially equal values of p_j/p_∞ may be obtained by comparing the boundaries for $\gamma_j = 1.400$ and 1.200 at $p_j/p_\infty \approx 1,300$ as shown in figure 7. (Actually, for $\gamma_j = 1.400$, $p_j/p_\infty = 1,346$ and for $\gamma_j = 1.200$, $p_j/p_\infty = 1,303$.) In spite of the short extent of the boundary for $\gamma_j = 1.200$, the comparison shown in figure 7 is sufficient to point up the large effect that γ_j has upon boundary shape at large pressure ratios.

Effect of γ_j for essentially equal initial inclination.- At low values of p_j/p_∞ (of the order of 10) the procedure of simulating a jet of one value of γ_j by a jet of another value of γ_j through duplication of the jet inclination of δ_j by changing the value of p_j/p_∞ is a useful artifice in many experimental investigations. An examination of the adequacy of this procedure at large pressure ratios is of interest. Figure 8 compares the boundary of the jet for $\gamma_j = 1.400$ with the

boundary for $\gamma_j = 1.667$, both having an initial inclination of about 60° but widely different values of p_j/p_∞ . (The value of p_j/p_∞ for $\gamma_j = 1.667$ is about 20 times that for $\gamma_j = 1.400$.) The comparison is sufficient to show that this procedure does not yield accurate simulation of the boundary at large pressure ratios and thus cannot be expected to give other than first-order simulation of interference effects. For extremely large values of p_j/p_∞ the curves of figure 2 serve to demonstrate that simulation by this procedure is impossible for the case of primary interest, namely, simulation of a jet having low γ_j by a jet having a higher γ_j (with significant differences in γ_j , of course, say of the order of 0.1 or more). For example, it is impossible for the jet of this study with $\gamma_j = 1.400$ to duplicate the value of δ_j for the jet with $\gamma_j = 1.200$ when the latter jet operates at values of p_j/p_∞ greater than about 10^4 .

Comments on Boundaries at Large Pressure Ratios

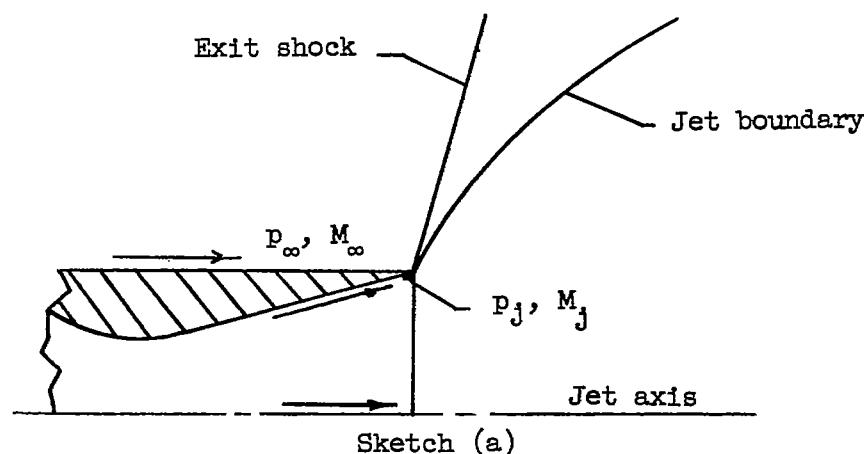
With Supersonic Ambient Stream

Hypothetical hypersonic vehicle.— Although the calculated boundaries of this study are for the jet exhausting into still air, it is apparent from these calculations that a rocket-propelled hypersonic vehicle may encounter serious jet interference problems if it encounters the high pressure ratios that are likely to occur at high altitudes. Some comments on the jet issuing from a hypothetical ground-launched hypersonic vehicle are thus considered in order.

Figure 9 presents an assumed speed-altitude variation of a hypothetical hypersonic vehicle. For simplicity a single rocket is assumed to provide power for the vehicle and the rocket is assumed to operate at design value at sea level (that is, at $p_j/p_\infty = 1$); in practical applications the value of p_j/p_∞ at sea level is usually less than 1.0 if the rocket is to encounter high altitudes.

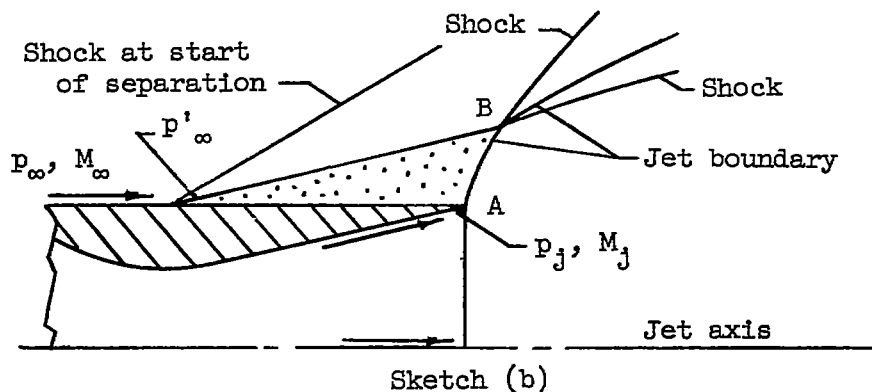
Variation of pressure ratio with altitude.— The variation of p_j/p_∞ with altitude was calculated with p_∞ assumed equal to the pressure at altitude and with the pressure at altitude varying according to the ICAO standard atmosphere (ref. 1) with extensions to higher altitudes. The value of p_j was assumed to be invariant with altitude. The

variation thus obtained is shown by the solid curve in figure 10 and represents the conditions shown in the following sketch:



It is important to note that the solid-line curve in figure 10 is independent of the value of M_∞ at altitude; the speed of the ambient flow could be zero at all altitudes or could vary in some arbitrary manner as in figure 9.

In order to examine the effect of speed-altitude variation of the hypothetical vehicle (fig. 9) on the initial inclination of the jet boundary δ_j , consideration must be given to the pressure rise through the shock in the ambient flow. For large pressure ratios separation will undoubtedly occur on the external surface ahead of the base because the boundary layer will not withstand a pressure rise of the magnitude necessary to turn the flow through the large initial deflections of the jet boundary. The following sketch probably represents a more realistic representation of the phenomena:



Little is known at present about the pressure rise associated with separation at hypersonic speeds; consequently two conditions have been examined. For one condition a pressure rise p'_∞/p_∞ corresponding to a 30° turning of the flow through an oblique shock at separation is assumed to occur; for the other condition, in order to have a quasi limiting condition, the pressure rise through a normal shock is assumed to have taken place ahead of the separated region. In the determination of the resulting values of p_j/p'_∞ , the pressure p'_∞ is assumed to hold throughout the separated region. The curves corresponding to the oblique shock with 30° turning and to the normal shock are shown in figure 10. Of course the portions of the curves at very low values of p_j/p'_∞ have no meaning since a 30° deflection of the external flow by the jet would be impossible at these low values. For large pressure ratios, however, the oblique-shock curve should give a reasonable first-order indication of the values of p_j/p'_∞ that would be encountered, and the fact that the normal-shock curve is not greatly removed from the oblique-shock curve is believed to indicate that values of δ_j calculated from the oblique-shock curve could not be greatly different from those that are experienced with practical configurations.

Variation of initial boundary inclination with altitude.— Since the curves of figure 10 are independent of γ_j , θ_N , and M_j , they may be applied to the nozzle of this study having $M_j = 2.5$, $\theta_N = 15^\circ$, and varying values of γ_j . Values of the initial inclination of the jet boundary δ_j for this nozzle have been determined with the aid of figures 2 and 10 and the results are shown in figure 11. The solid-line curves are for $M_\infty = 0$, and the dashed-line curves are for the speed-altitude variation of figure 9 with the oblique-shock separation of the boundary layer. Although only the curves for $\gamma_j = 1.200$ may be considered applicable to the rocket-propulsion unit of the hypothetical vehicle, the curves for the other values of γ_j have been included to point up the effect of γ_j and for possible information on the behavior of jets on reaction controls. Again the lower portions of the dashed-line curves (small δ_j) have no meaning. The difference between the solid-line curve and the dashed-line curve at a particular γ_j shows the effect that the presence of supersonic ambient flow, defined according to figure 9 and with separation ahead of the base, has in reducing the initial deflection of the boundary. As the extremely large pressure ratios of high altitude are approached (fig. 11), the effects of the ambient flow may be readily deduced from these curves to be

secondary in determining the value of δ_j . Of particular importance is the indication that feasible rocket-propelled hypersonic vehicles may encounter within their range of operation initial inclinations of the boundary approaching and exceeding 90° ; consequently, large regions of separated flow, together with large aerodynamic and possible aerothermal interference effects, may occur.

Remarks on boundary shape.- The indication that the effects of the ambient flow are secondary at extremely large pressure ratios in determining the value of δ_j does not imply that the shape of the boundary will not be significantly affected by the ambient flow at lower pressure ratios. No reason is apparent why the procedure employed at low pressure ratios for determining the shape of the portion of the jet boundary that bounds the region of separation (from A to B in sketch (b)) should not be useful at large pressure ratios; in this procedure this portion of the boundary is determined by employing the boundary of the jet exhausting into still air at a pressure ratio equal to p_j/p'_∞ . However, at point B of sketch (b), where the separated region ends and the jet flow and ambient flow interact directly, a large and abrupt turning of the boundary may be expected at large pressure ratios and hypersonic speeds, if the flow deflections accompanying separation at these speeds are of the order of 30° (turbulent boundary layer preceding separation), as seems likely on the basis of available experimental information. Beyond point B the ambient flow will have significant influence on the boundary shape in the same manner as it does at low pressure ratios and supersonic speeds.

CONCLUDING REMARKS

Calculations have been made of the initial portion of the boundary of axisymmetric free jets exhausting into still air when the ratio of jet static pressure to stream static pressure is high. The jet Mach number of these calculations was 2.5 and the semidivergence angle of the nozzle was 15° . The calculations covered static-pressure ratios from about 60 to 42,000 and ratios of specific heats of 1.200, 1.400, and 1.667. The results indicate the enormous size that the free jet may attain at large pressure ratios and point up the large effects of the ratio of specific heats at large pressure ratios. A cursory examination of the behavior of the propulsive jet on a hypothetical rocket-propelled hypersonic vehicle indicates that feasible hypersonic vehicles may encounter within their range of operation initial inclinations of the free-jet boundary approaching and exceeding 90° . Consequently,

large regions of separated flow may occur on such vehicles, together with large aerodynamic and possible aerothermal interference effects.

Langley Aeronautical Laboratory,
National Advisory Committee for Aeronautics,
Langley Field, Va., October 14, 1957.

REFERENCE

1. Anon.: Standard Atmosphere - Tables and Data for Altitudes to 65,800 Feet. NACA Rep. 1235, 1955. (Supersedes NACA TN 3182.)

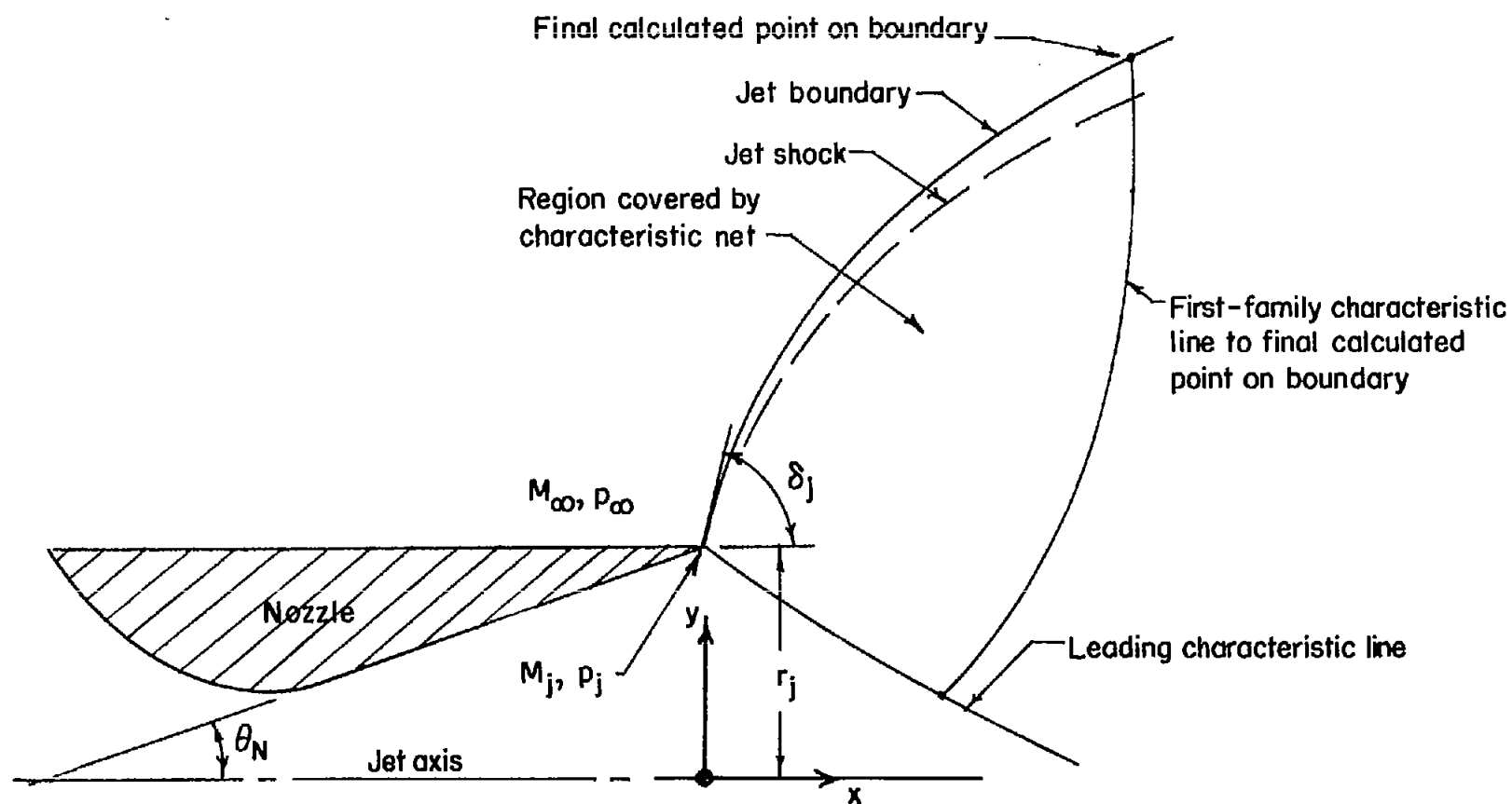


Figure 1.- Sketch of jet exhausting from conically divergent nozzle into still air showing pertinent details and parameters.

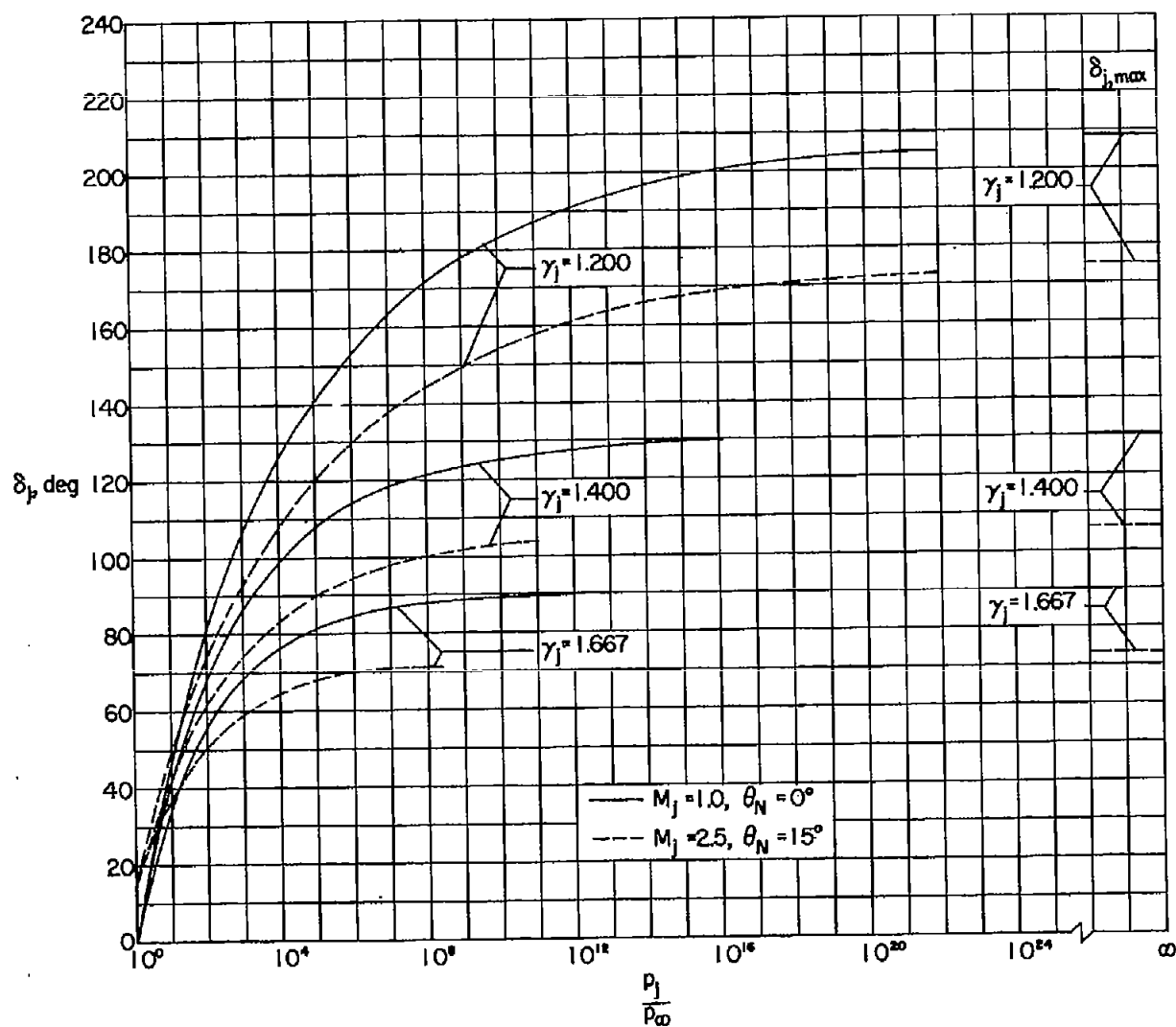
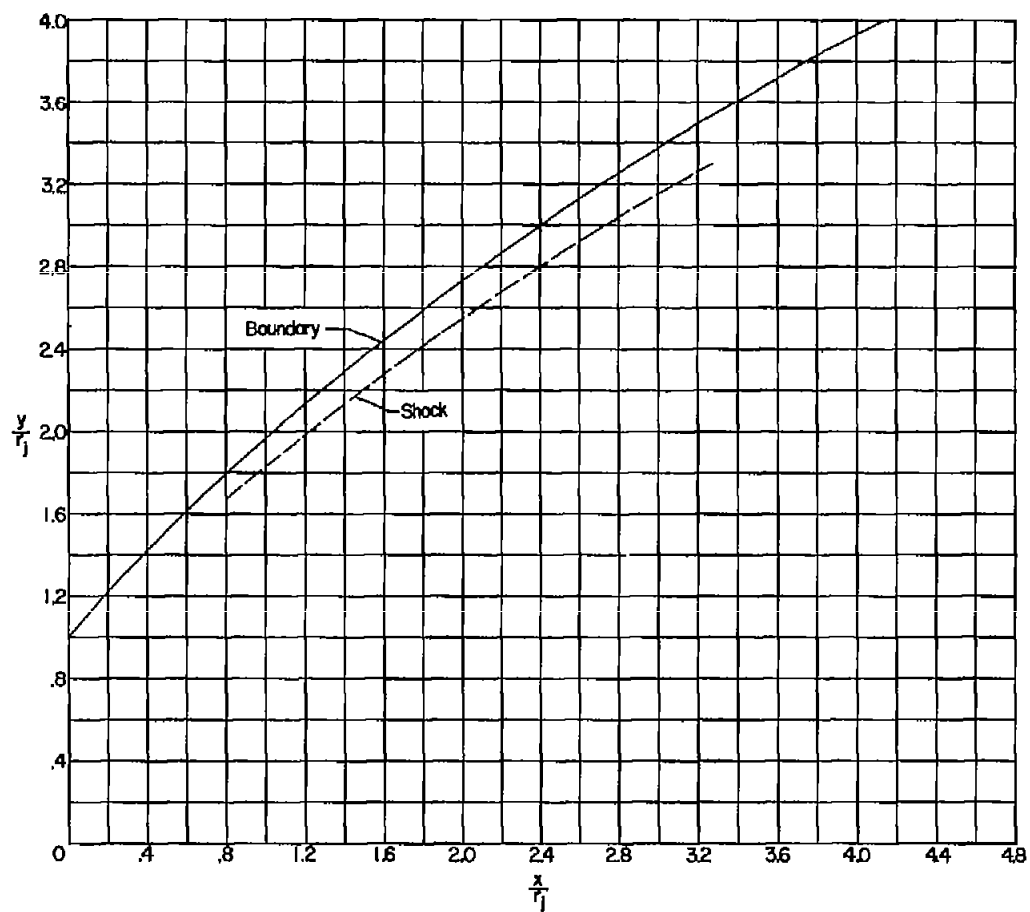
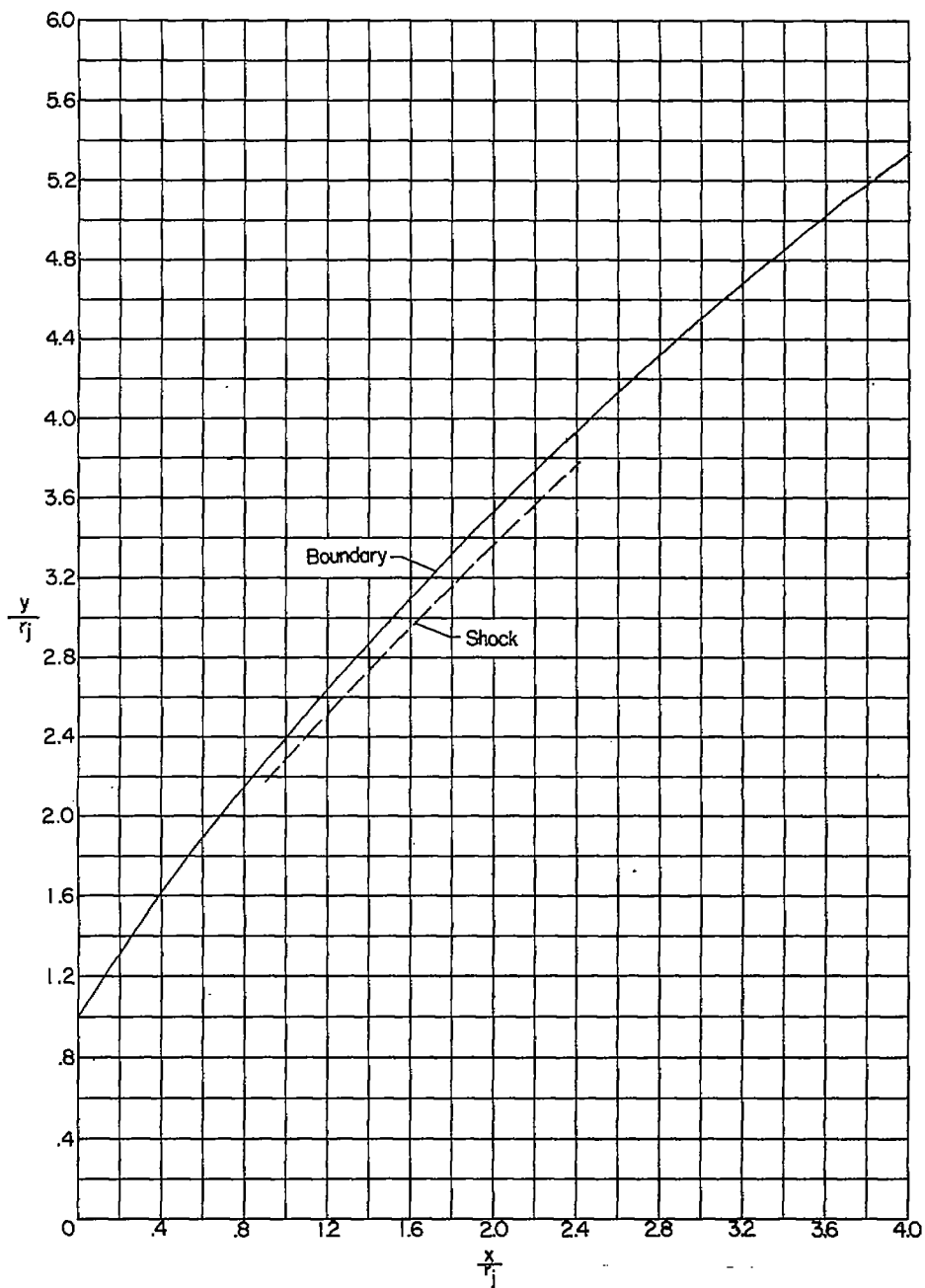


Figure 2.- Variation of the initial inclination of the free-jet boundary with jet static-pressure ratio for jets exhausting into still air.



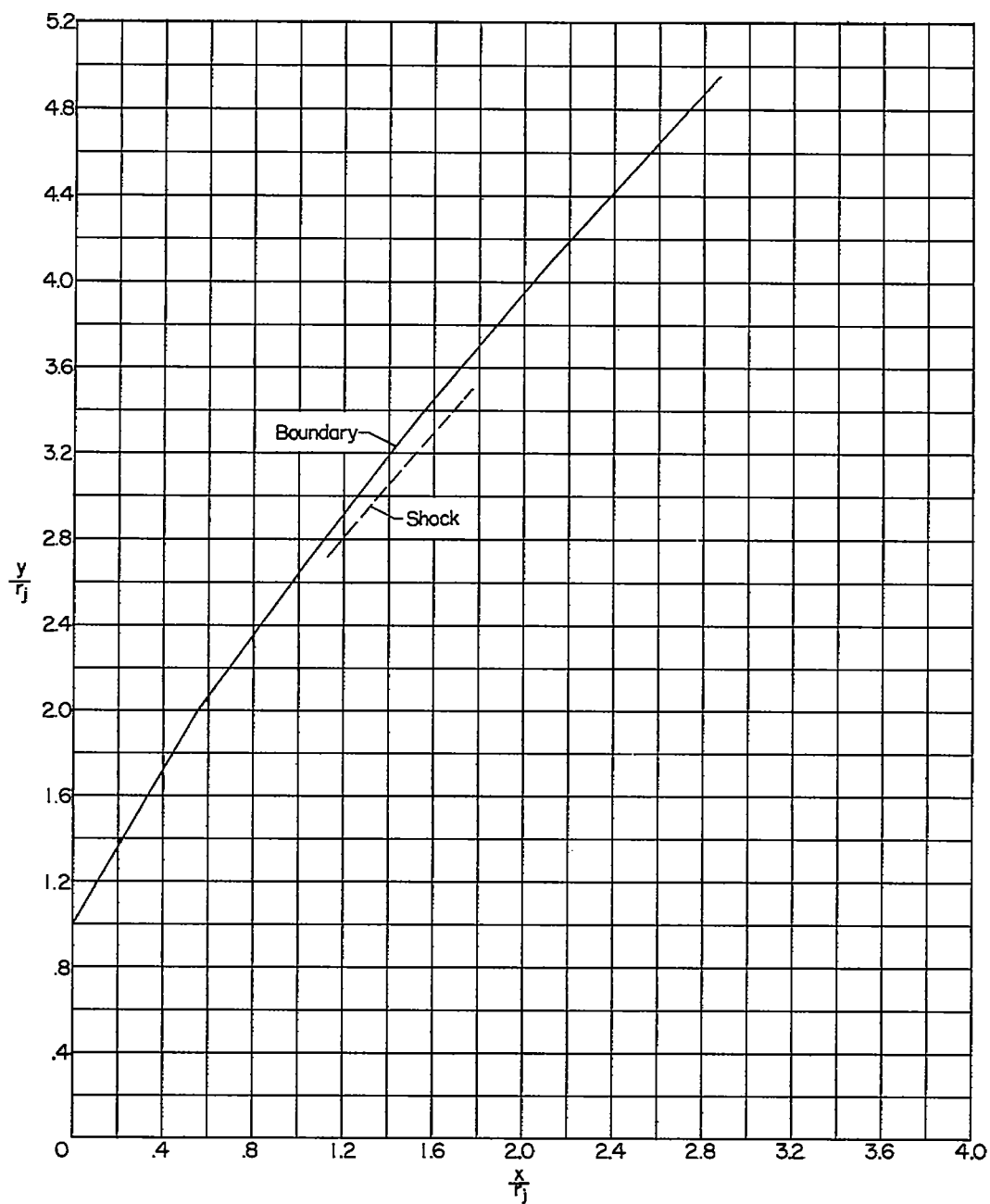
(a) $\frac{p_j}{p_\infty} = 59.92; \delta_j = 48.55^\circ.$

Figure 3.- Calculated boundaries and jet shocks for jet exhausting into still air with $\gamma_j = 1.667$, $M_j = 2.5$, and $\theta_N = 15^\circ$.



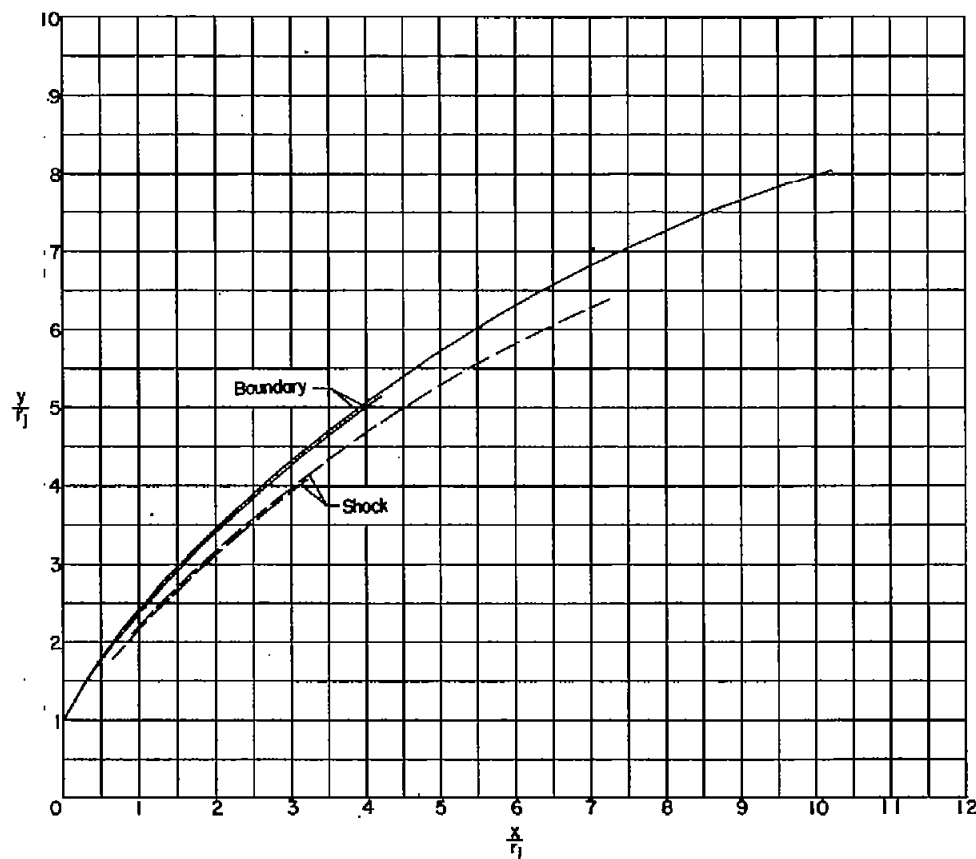
(b) $\frac{p_j}{p_\infty} = 569.2; \delta_j = 57.72^\circ.$

Figure 3.- Continued.



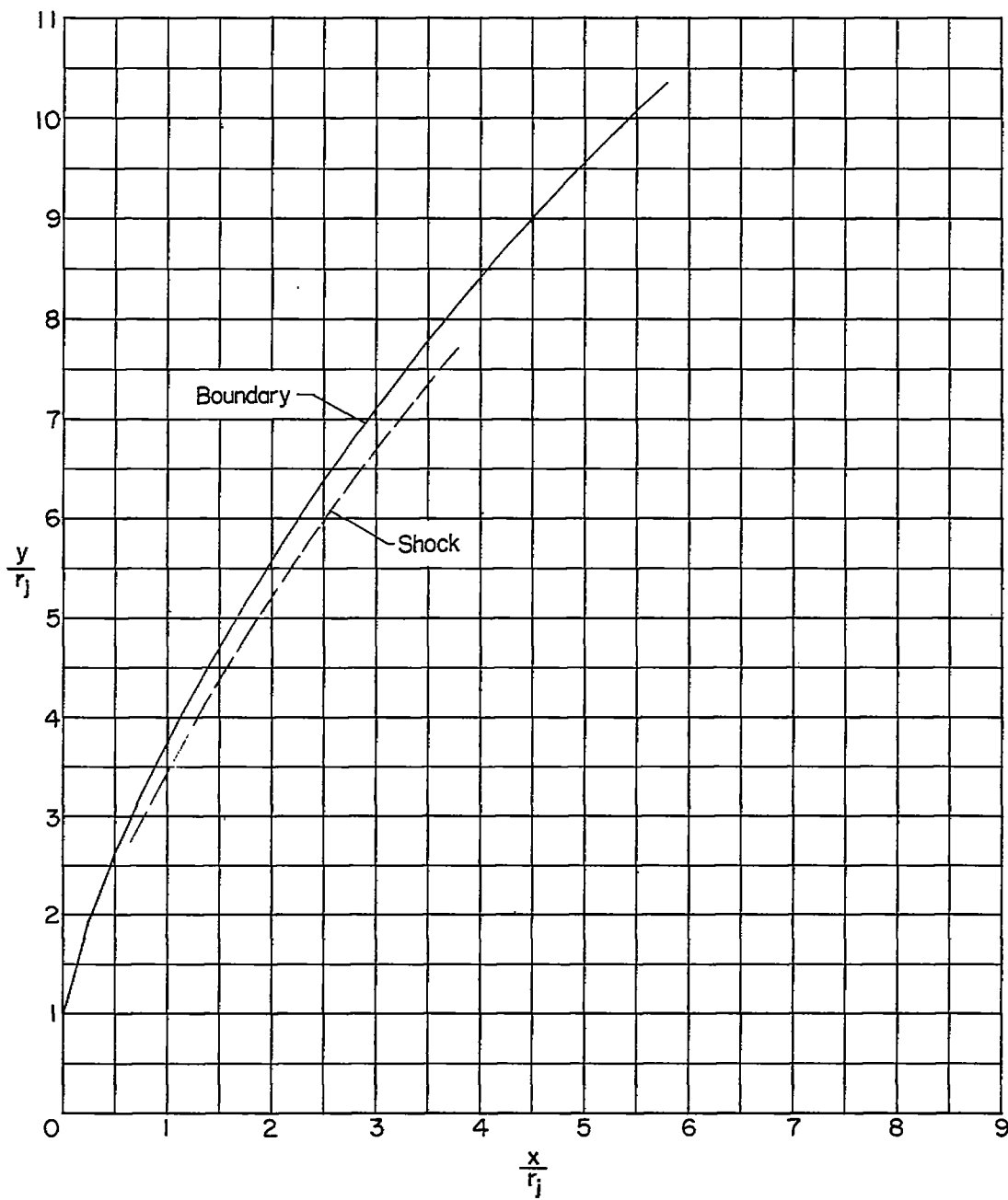
(c) $\frac{p_j}{p_\infty} = 1.618; \delta_j = 60.74^\circ.$

Figure 3.- Concluded.



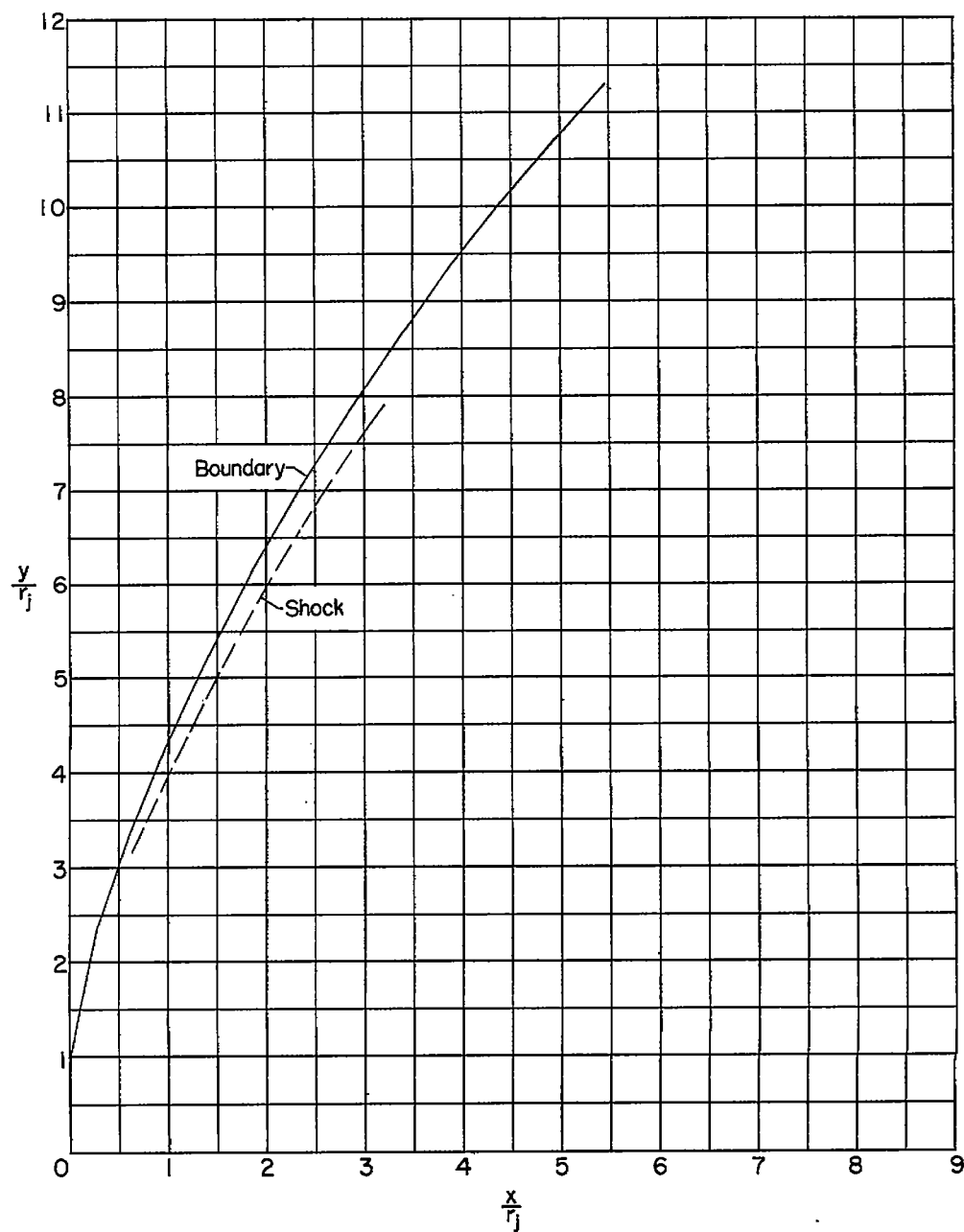
(a) $\frac{p_j}{p_\infty} = 81.94$; $\delta_j = 60.02^\circ$.

Figure 4.- Calculated boundaries and jet shocks for jet exhausting into still air with $\gamma_j = 1.400$, $M_j = 2.5$, and $\theta_N = 15^\circ$. Longer boundary and shock correspond to greater spacing between points on leading characteristic than for shorter boundary and shock (see text).



(b) $\frac{p_j}{p_\infty} = 1.346$; $\delta_j = 75.59^\circ$.

Figure 4.- Continued.



(c) $\frac{p_j}{p_\infty} = 2,692; \delta_j = 78.53^\circ.$

Figure 4.- Concluded.

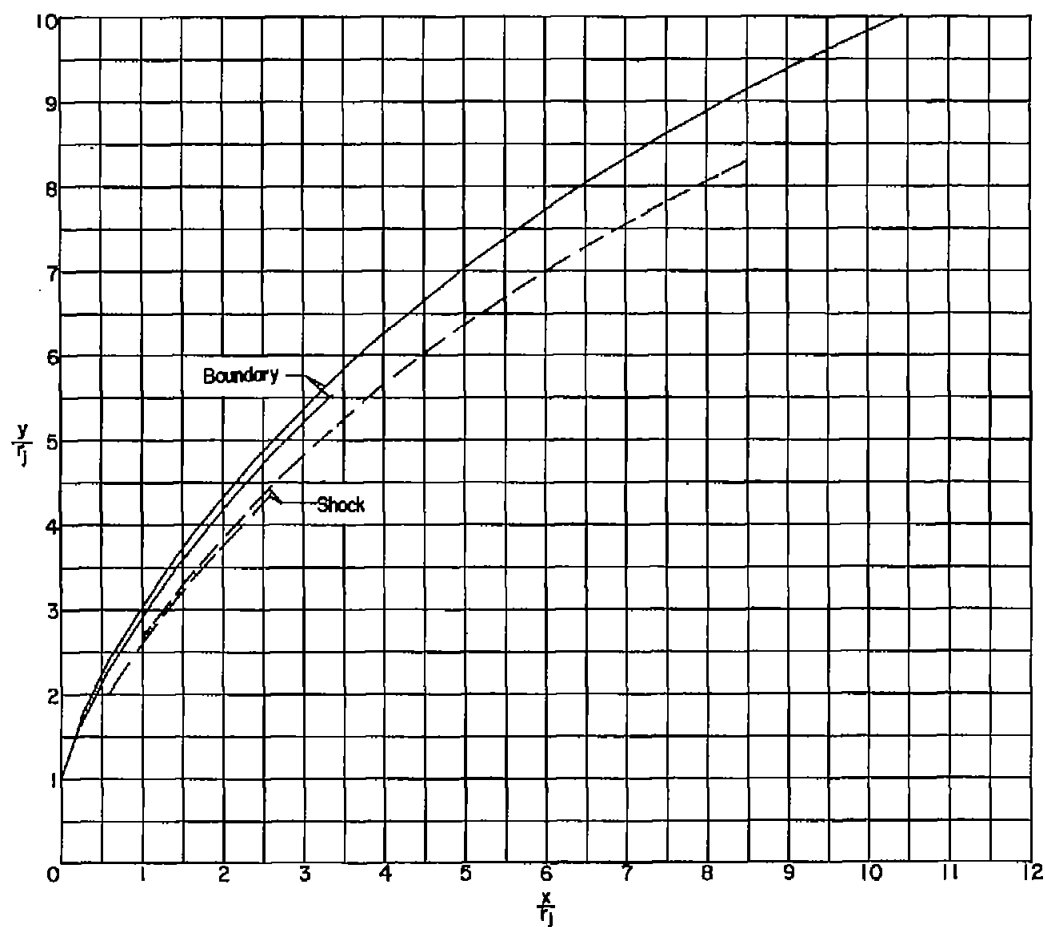
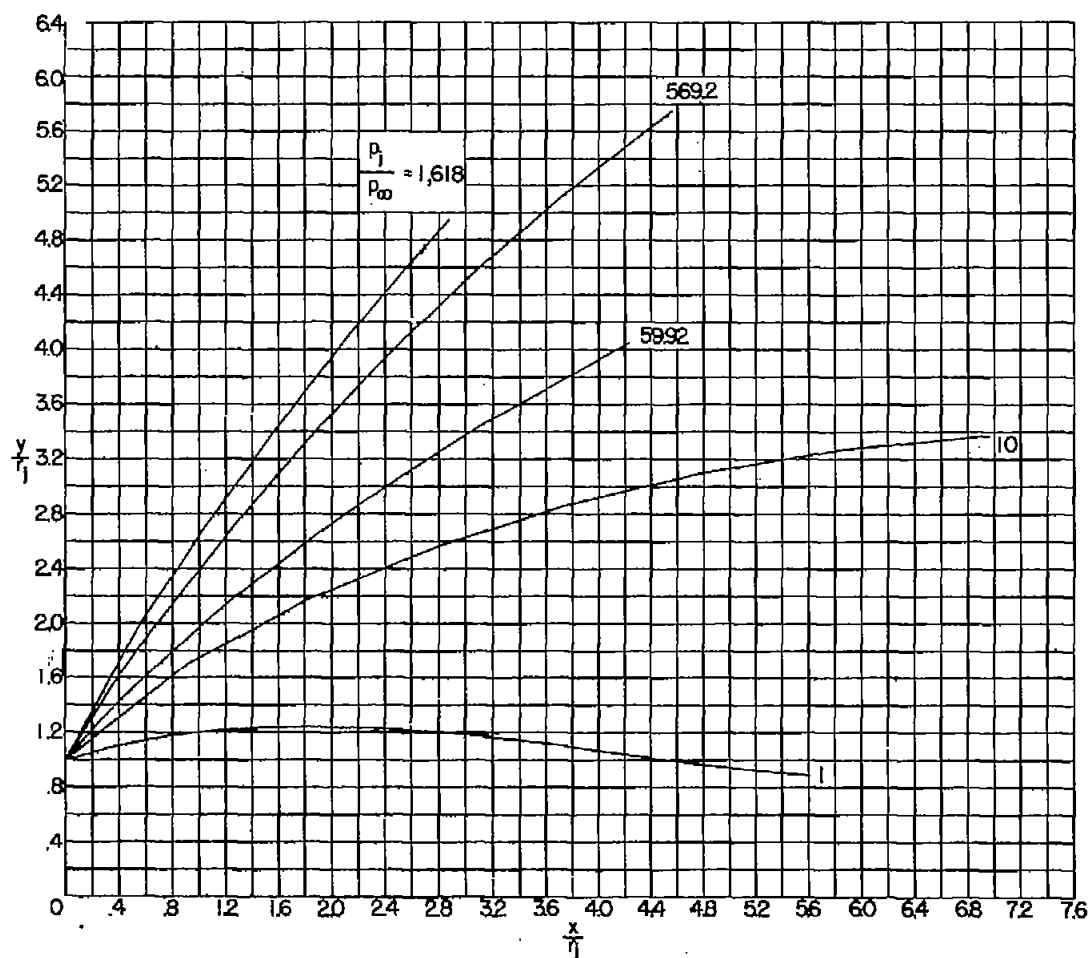


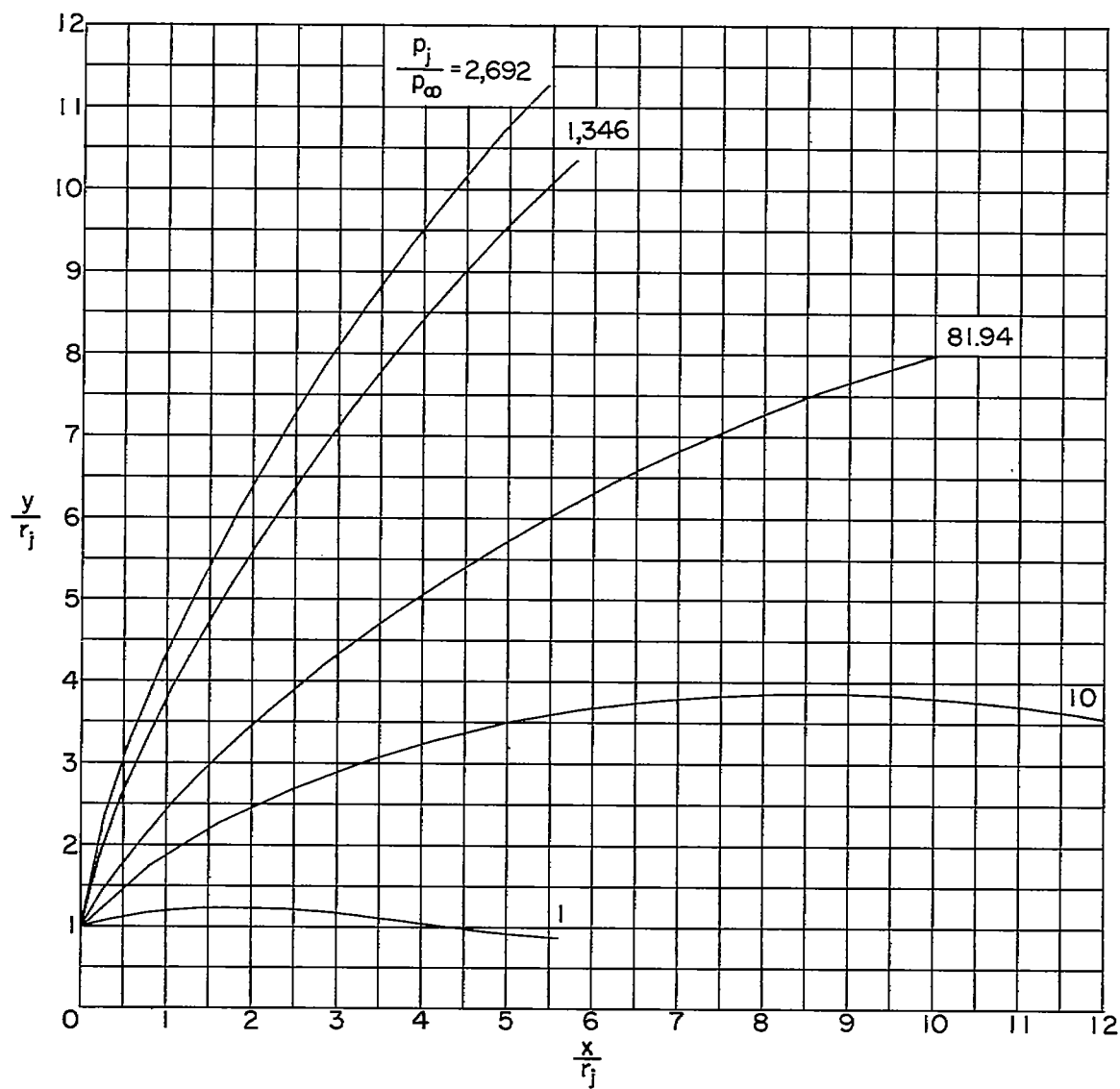
Figure 5.- Calculated boundary and jet shock for jet exhausting into still air at $\frac{P_j}{P_\infty} = 76.58$

with $\gamma_j = 1.200$, $M_j = 2.5$, and $\theta_N = 15^\circ$. Longer boundary and shock correspond to greater spacing between points on leading characteristic than for shorter boundary and shock (see text).



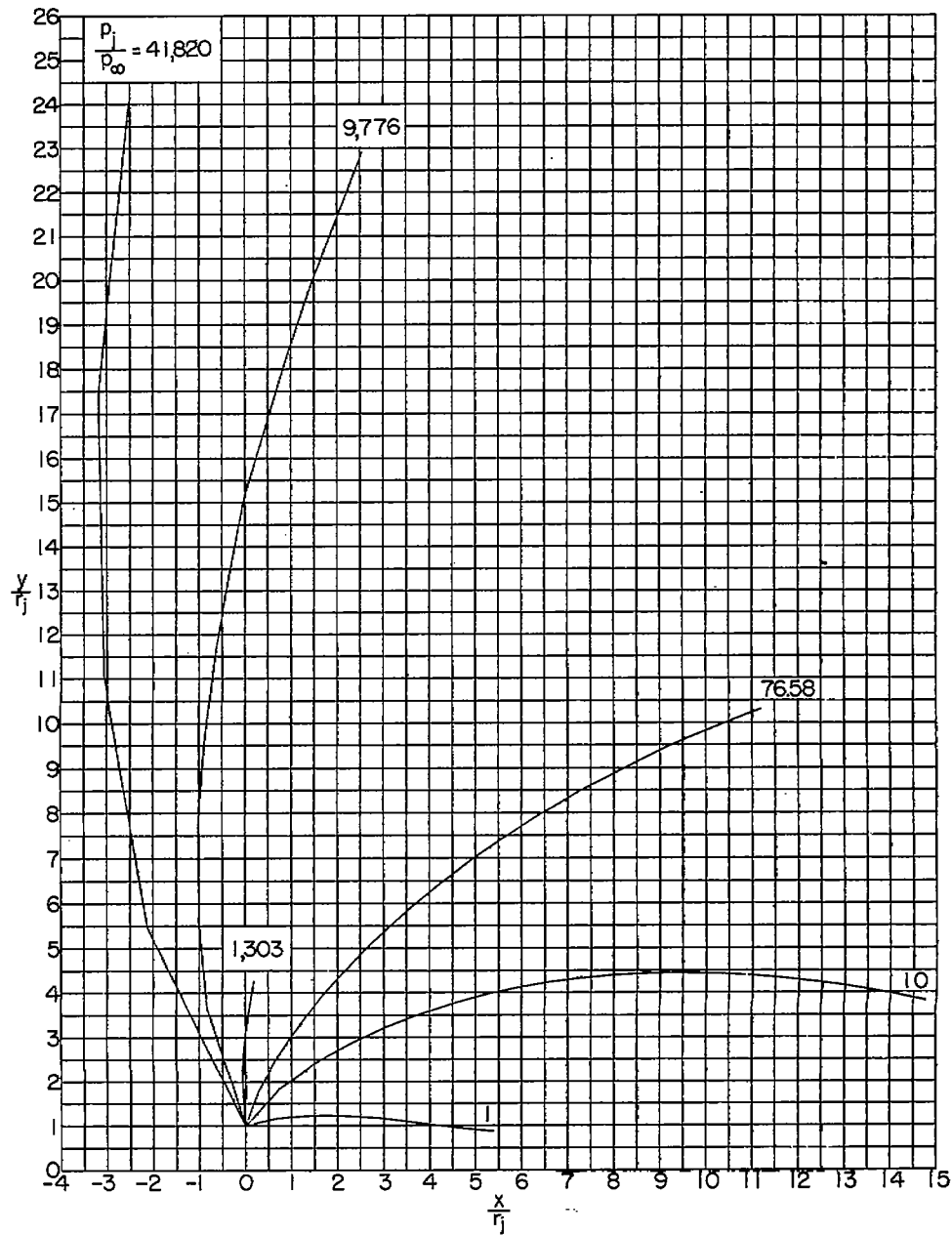
(a) $\gamma_j = 1.667$.

Figure 6.- Composite presentation of calculated boundaries for jet exhausting into still air with $M_j = 2.5$ and $\theta_N = 15^\circ$.



(b) $\gamma_j = 1.400$.

Figure 6.- Continued.



(c) $\gamma_j = 1.200$.

Figure 6.- Concluded.

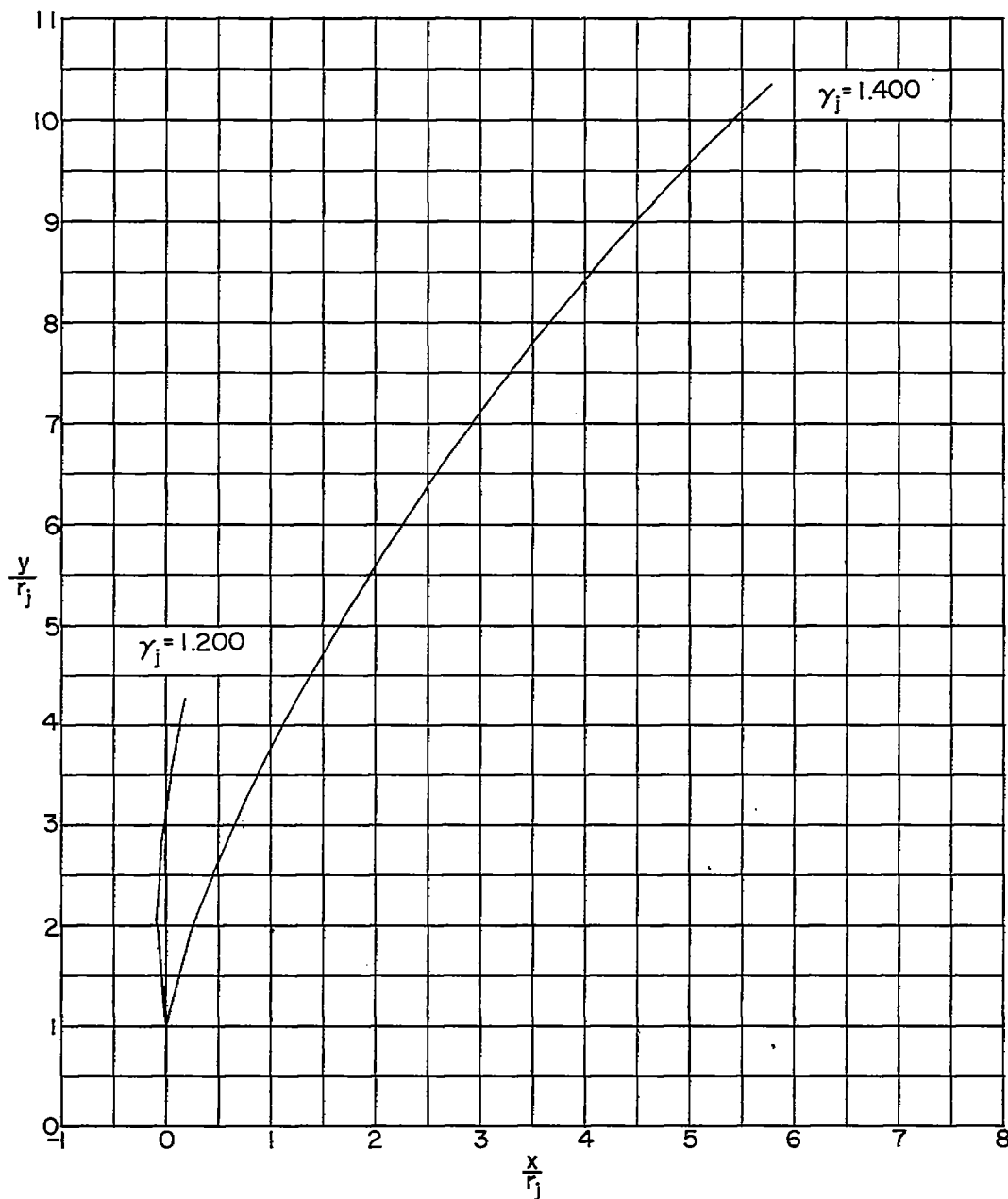


Figure 7.- Example of the effect of γ_j at large pressure ratios upon shape of boundary for similar pressure ratios. Jet exhausting into still air; $M_j = 2.5$; $\theta_N = 15^\circ$; $\frac{p_j}{p_\infty} \approx 1,300$.

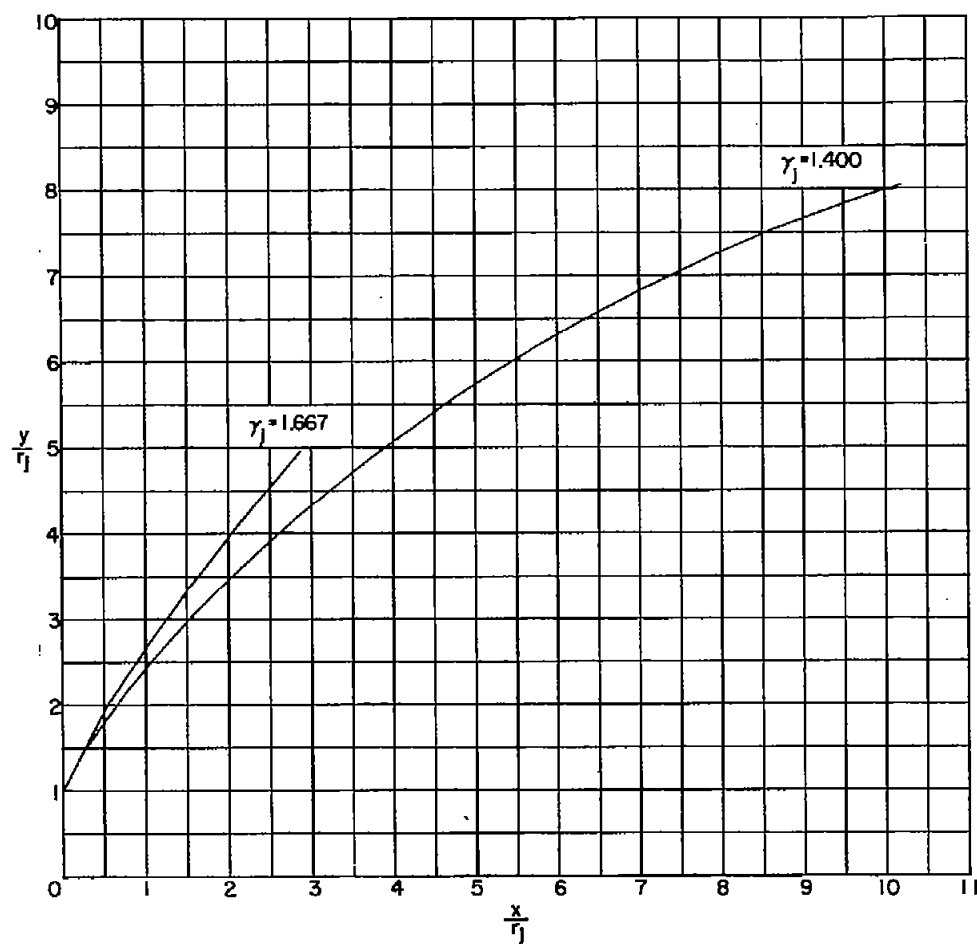


Figure 8.- Example of effect of γ_j at large pressure ratios upon shape of boundary for similar initial inclinations of boundary. Jet exhausting into still air; $M_j = 2.5$; $\theta_N = 15^\circ$; $\delta_j \approx 60^\circ$.

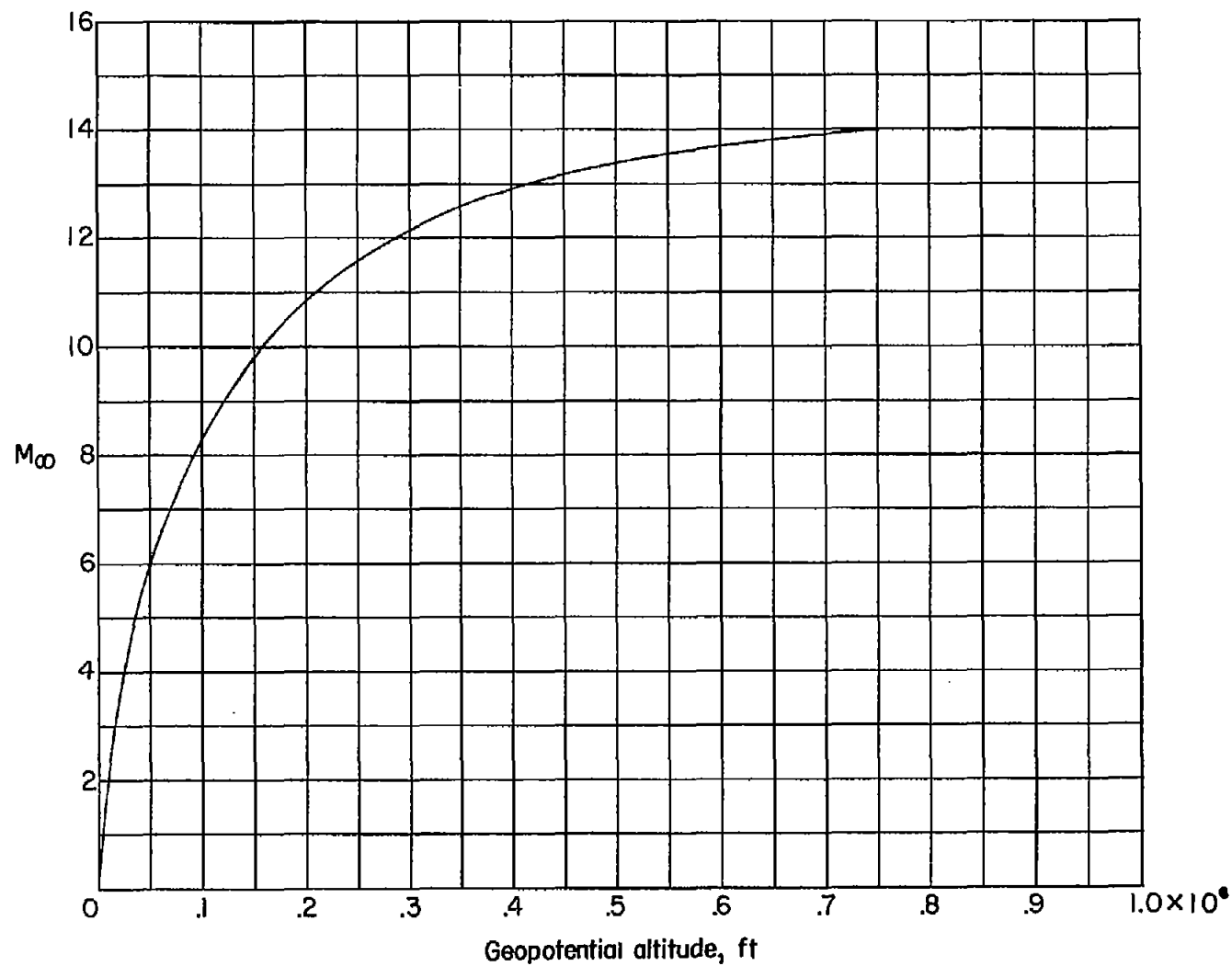


Figure 9.- Assumed Mach number altitude variation of hypothetical vehicle.

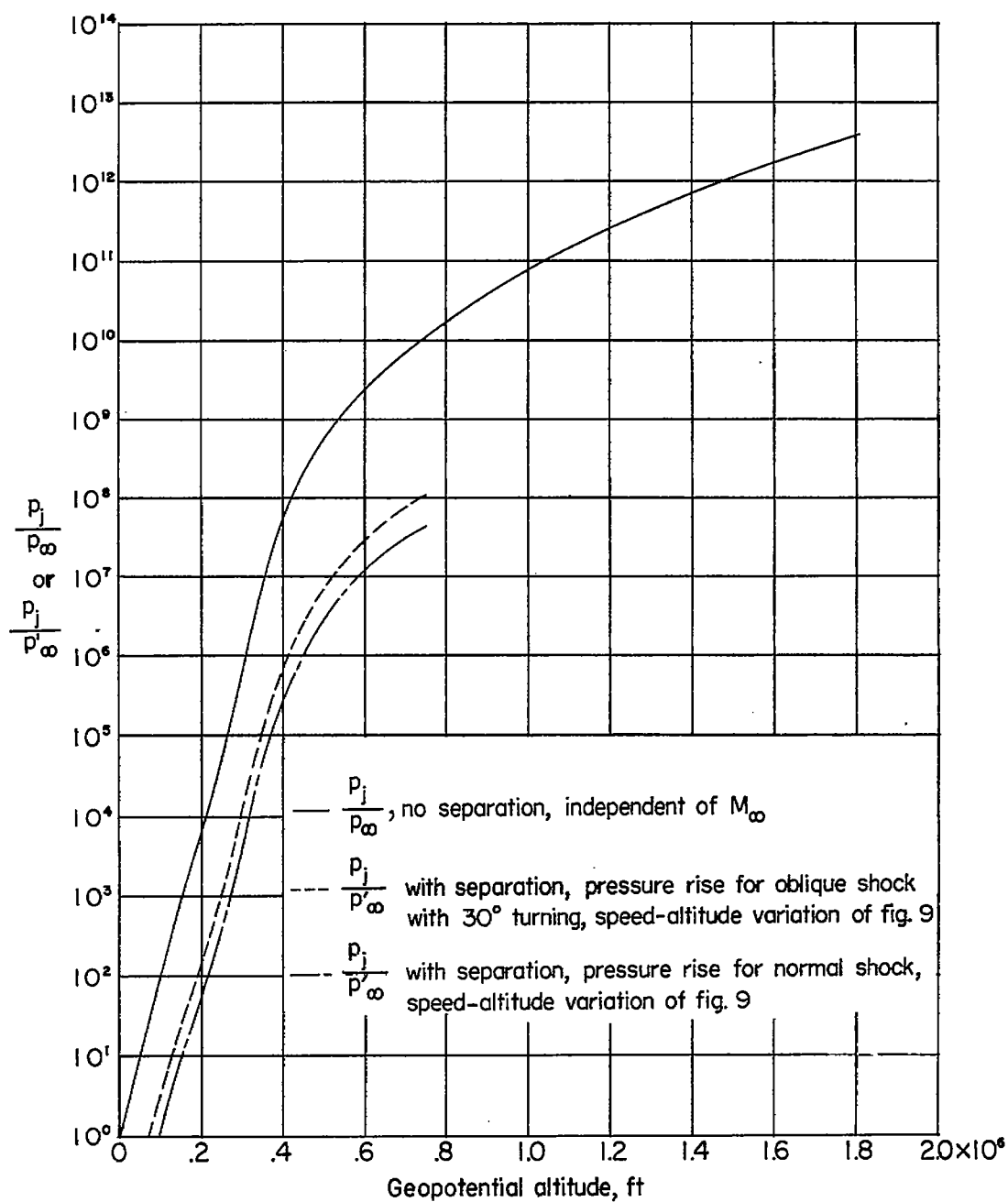


Figure 10.- Variation of pressure ratio with altitude. For all curves $\frac{p_j}{p_0} = 1$ at sea level, p_j is invariant with altitude, and p_∞ equals pressure at altitude.

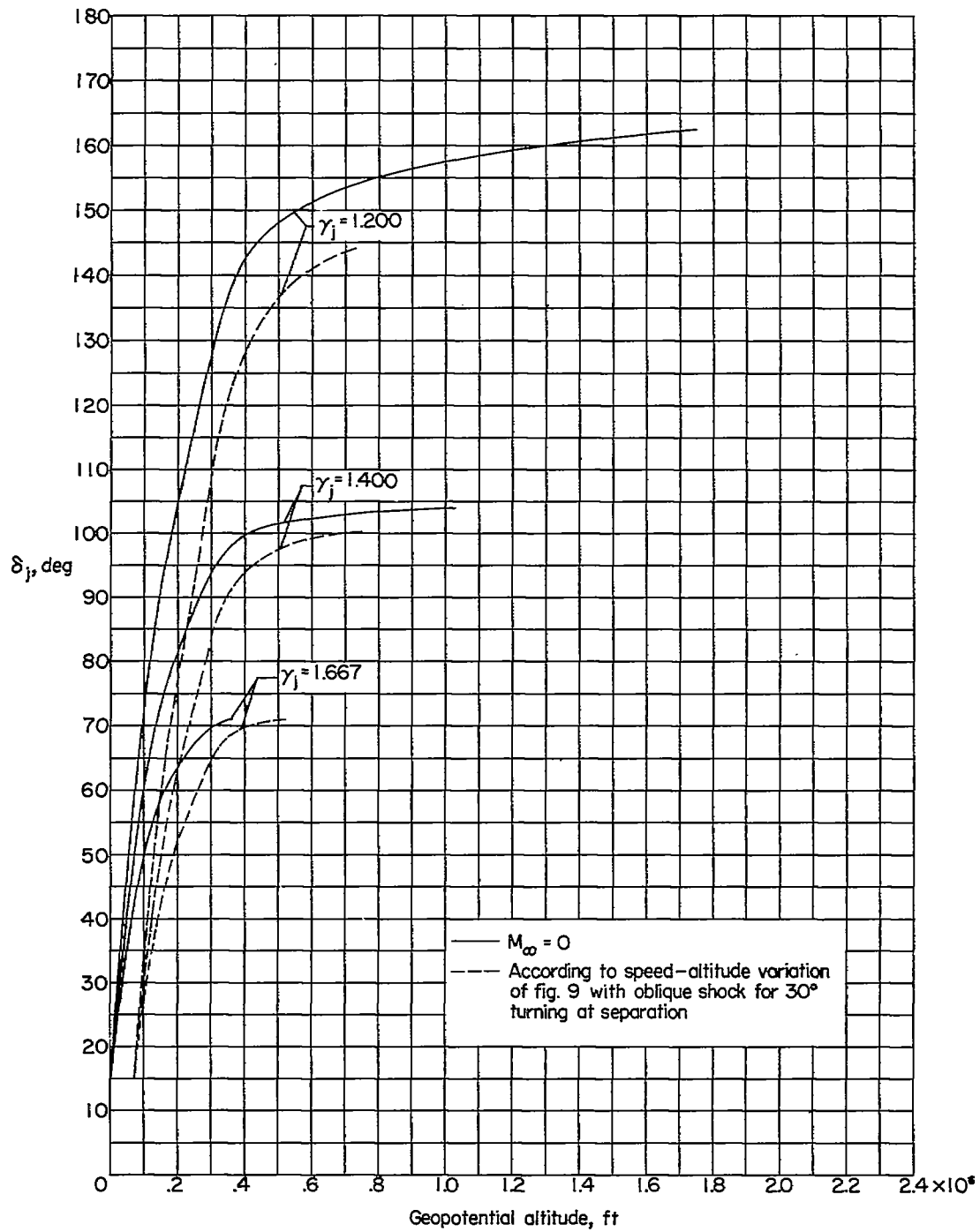


Figure 11.- Variation of initial inclination of boundary with altitude.
 $M_j = 2.5$; $\theta_N = 15^\circ$.